International Journal of Automotive Technology, Vol. 19, No. 2, pp. 291–299 (2018)
DOI 10.1007/s12239–018–0028–x

Copyright © 2018 KSAE/ 101–10
pISSN 1229–9138/ eISSN 1976–3832

STRUCTURAL OPTIMIZATION FOR ROOF CRUSH TEST USING AN ENFORCED DISPLACEMENT METHOD

Wook-Han Choi[1)], Youngmyung Lee[2)], Jong-Min Yoon[1)], Yong-Ha Han[3)] and Gyung-Jin Park[2)*]

[1)]Department of Mechanical Engineering, Hanyang University, Seoul 04763, Korea
[2)]Department of Mechanical Engineering, Hanyang University, Gyeonggi 15588, Korea
[3)]Advanced Safety CAE Group, Hyundai Motor Group, 150 Hyundaiyeonguso-ro, Namyang-eup, Hwaseong-si, Gyeonggi 18280, Korea

(Received 3 April 2017; Revised 28 June 2017; Accepted 17 July 2017)

ABSTRACT–A roof crush test has been utilized to reduce passengers' injuries from a vehicle rollover. The Federal Motor Vehicle Safety Standards (FMVSS) 216 and the Insurance Institute for Highway Safety (IIHS) perform actual vehicle tests and evaluate the vehicle's ratings. Nonlinear dynamic response structural optimization can be employed not only for achievement of a high rating but also minimization of the weight. However, the technique needs a huge computation time and cost because many nonlinear dynamic response analyses are required in the time domain. A novel method is proposed for nonlinear dynamic response structural optimization regarding the roof crush test. The process of the proposed method repeats the analysis domain and the design domain until the convergence criteria are satisfied. In the analysis domain, the roof crush test is simulated using a high fidelity model of nonlinear dynamic finite element analysis. In the design domain, a low fidelity model of linear static response structural optimization is utilized with enforced displacements that come from the analysis domain. Correction factors are employed to compensate the differences between a nonlinear dynamic analysis response and a linear static analysis response with enforced displacement. A full-scale vehicle problem is optimized with a constraint on the rigid wall force from the analysis in the design domain.

KEY WORDS : Roof crush test, Structural optimization, FMVSS 216

1. INTRODUCTION

The National Highway Traffic Safety Administration (NHTSA) reported that vehicle rollover accidents show a higher fatality rate than other types of vehicle accidents (Strashny, 2007). In a frontal crash, a front crumple zone absorbs almost all the impact energy. In rollover accidents, there is no specific vehicle that absorbs the impact energy between the roof and passengers. Therefore, impact loads are directly transmitted to passengers and cause fatal injuries (Kahane, 1989; Rechnitzer *et al*., 1996). NHTSA has defined the strength requirements for the roof compartment of passenger vehicles through FMVSS 216 (Cho and Han, 2012; Mao *et al*., 2007; Seo *et al*., 2016). In industries, roof crush optimization has been employed to satisfy the strength requirements. The roof crush analysis is facilitated due to the advance in technology with regard to nonlinear dynamic response finite element analysis of large scale structures. The structural optimization that uses nonlinear dynamic response analysis is nonlinear dynamic response structural optimization.

It is well-known that the conventional gradient based optimization is extremely expensive for nonlinear dynamic response optimization of large scale structures. Generally, a metamodel technique is adopted for nonlinear dynamic structural optimization of practical examples (Jang *et al*., 2016; Lee *et al*., 2013; Lim *et al*., 2015; Niknejad *et al*., 2015; Pan and Zhu, 2011; Tey *et al*., 2016; Wang *et al*., 2016; Yun *et al*., 2014). A metamodel is easy to handle and various responses can be considered. However, the quality of the optimum is dependent on the reliability of the metamodel. Hence, many samplings are needed to build a reliable metamodel that is directly related to cost. To overcome the above difficulties, the equivalent static loads method (ESLM) was proposed (Choi and Park, 1999). ESLM has two domains that are the analysis domain and the design domain. Nonlinear dynamic analysis is carried out in the analysis domain while linear static response structural optimization is performed in the design domain by using the equivalent static loads (ESLs) that are calculated by the displacement vectors from the nonlinear dynamic response analysis. ESLM has been widely applied and validated through many practical examples (Green *et al*., 2009; Hong *et al*., 2010; Jang *et al*., 2012; Jeong *et al*., 2010; Kim and Park, 2010; Lee and Park, 2015; Müllerschön *et al*., 2013; Park, 2011; Yi *et al*., 2012).

Jeong *et al*. (2008) presented a roof crush optimization using a full scale vehicle to improve the strength

*Corresponding author. e-mail: gjpark@hanyang.ac.kr

requirements of the roof crush test. They utilized the ESLM and compared the results with those from the metamodel based optimization. ESLM obtained excellent results compared to the metamodel based optimization. The optimal value of the objective function of ELSM was better than that of the metamodel based method with a smaller number of roof crush analyses. However, they could not directly consider the strength requirement such as the rigid wall force. The reason is that the rigid wall force cannot be changed in the linear static response structural optimization process. Therefore, the design constraint of the strength requirement was converted to a displacement constraint and the force (rigid wall force)-displacement target curve was found by a trial-and-error process. The roof crush optimization using ESLM is reviewed in Section 4.2.

In this research, a novel method for roof crush optimization is proposed. The proposed method uses the paradigm of ESLM working in two domains. In the design domain, roof crush analysis is carried out and displacements are extracted in the contacted area between the roof and the rigid wall. In the design domain, linear static response structural optimization is carried out using the extracted displacements as enforced displacements (Lee *et al*., 2016). The design constraint of the rigid wall force in a roof crush test is converted to a constraint on the reaction force at the boundary condition in linear static response structural optimization. The differences between the rigid wall force from nonlinear analysis and the reaction force of the boundary condition from linear analysis are calibrated using correction factors. The proposed method is validated through a small scale roof crush example and expanded to a full scale vehicle. To ensure the convergence of the proposed method, the process starts from the feasible region as well as the infeasible region. The optimization results are compared with those from ESLM. The roof crush analysis is performed by LS-DYNA (Livermore Software Technology Co., 2007) and linear static response structural optimization is solved by NASTRAN (MSC Software Co., 2013).

2. PROPOSED METHODFOR ROOF CRUSH OPTIMIZATION

The governing equation of nonlinear dynamic analysis is as follows:

$$\mathbf{M}(\mathbf{b})\ddot{\mathbf{z}}_{\mathrm{N}}(t)+\mathbf{C}(\mathbf{b})\dot{\mathbf{z}}_{\mathrm{N}}(t)+\mathbf{K}_{\mathrm{N}}(\mathbf{b},\mathbf{z}_{\mathrm{N}}(t))\mathbf{z}_{\mathrm{N}}(t)=\mathbf{f}(t) \quad , \ t=1,\ldots,l \tag{1}$$

where **M**, **C** and **K** are the mass matrix, damping matrix and stiffness matrix, respectively. $\ddot{\mathbf{z}}_{\mathrm{N}}$, $\dot{\mathbf{z}}_{\mathrm{N}}$ and $\mathbf{z}_{\mathrm{N}}$ are the acceleration vector, the velocity vector and the displacement vector, respectively. **f** is the external load vector. The subscript N denotes the properties of nonlinear dynamic analysis. *l* denotes the number of time steps. Since the roof crush test is a quasi-static test, acceleration and velocity are quite small. Thus, the effect of damping and mass is small. We made a hypothesis in that the rigid wall force is quite similar to the sum of the reaction forces at the boundary condition in the roof crush test. Then using the enforced displacements in linear static response analysis, the sum of the reaction force at the boundary condition is similar to the rigid wall force of the roof crush test. To validate the hypothesis, a simplified roof crush finite element (FE) model is made as shown in Figure 1. The top of the tapered FE model is smaller than the bottom part for the boundary condition, and two reinforcements are located in the middle of the structure. The rigid wall crushes the simplified model at a velocity of 2.233 mm/s in the z-direction. All the degrees of freedom are fixed at the bottom part.

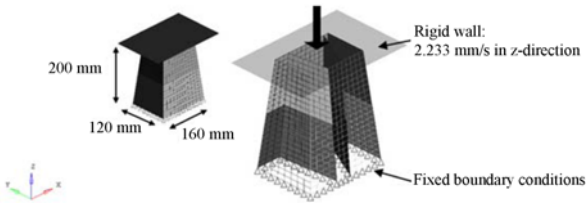

Figure 1. Simplified finite element model for the roof crush test.

First, the rigid wall force and the sum of the reaction forces at the boundary condition are compared in the nonlinear dynamic response analysis. As shown in Figure 2, the profiles of the two forces are very similar because they are from quasi-static analyses. Second, the rigid wall force from nonlinear dynamic analysis and the sum of the reaction forces at the boundary condition from linear static analysis with enforced displacements are compared. As shown in Figure 2, the rigid wall force curve can be divided into a) Linear range, b) Peak range, and c) Nonlinear range. Three time steps are selected in each range. Table 1 shows the comparison results. The linear and peak ranges show small errors and the nonlinear range shows 192.0 % error. When the deformation is large, the enforced displacement

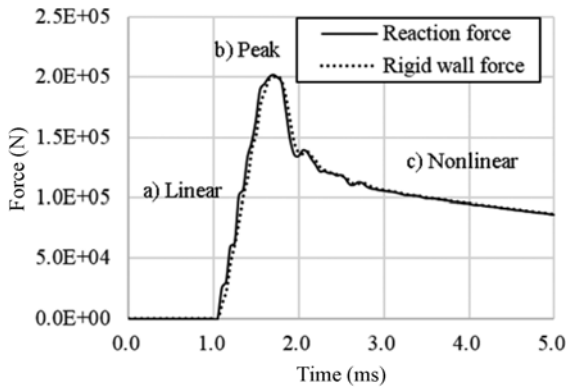

Figure 2. Comparison between sum of the reaction forces and rigid wall force.

Table 1. Comparison between the sum of the reaction forces and the rigid wall force.

	Rigid wall force	Sum of the reaction forces	Error (%)
a) Linear (t = 1.299 ms)	1.226E+5	1.270E+5	3.6 %
b) Peak (t = 1.748 ms)	2.008E+5	2.160E+5	7.6 %
c) Nonlinear (t = 2.149 ms)	1.329E+5	3.881E+5	192.0 %

is quite large and the reaction force at the boundary condition is very large in linear static analysis. As mentioned earlier, the reaction force in linear static analysis corresponds to the rigid wall force in nonlinear dynamic analysis. The rigid wall force can be smaller than the reaction force due to the plastic deformation. In order to correct the difference between the two forces, the correction factor technique is utilized. Kim and Park (2010) proposed the correction factor technique that is determined by the ratio between nonlinear dynamic analysis response and linear static analysis response with ESLs. In this research, the ratio is named as correction factor α and the sum of the reaction forces is calibrated as follows:

$$\alpha = \frac{\mathrm{F}_{\text{rigid wall force}}\big|_{t=\text{arbitrary}}}{\sum \mathrm{F}_{\text{reaction force}}(\mathbf{z}_{\text{N,roof}}\big|_{t=\text{arbitrary}})} \tag{2}$$

$$\sum \hat{\mathrm{F}}_{\text{reaction force}}(\mathbf{z}_{\text{N,roof}}\big|_{t=\text{arbitrary}}) = \sum \mathrm{F}_{\text{reaction force}}(\mathbf{z}_{\text{N,roof}}\big|_{t=\text{arbitrary}}) \times \alpha \tag{3}$$

where $\mathrm{F}_{\text{rigid wall force}}\big|_{t=\text{arbitrary}}$ is the reaction force of the rigid wall in nonlinear dynamic analysis at an arbitrary time and $\sum \mathrm{F}_{\text{reaction force}}$ is the sum of the reaction forces of linear static analysis using the enforced displacements $\mathbf{z}_{\text{N,roof}}\big|_{t=\text{arbitrary}}$ at the boundary conditions. The corrected sum of the reaction forces $\sum \hat{\mathrm{F}}_{\text{reaction force}}$ is calculated in Equation (3). Therefore, $\sum \hat{\mathrm{F}}_{\text{reaction force}}$ has exactly the same value as the rigid wall force at an arbitrary time from the roof crush analysis. The schematic view of the proposed method is illustrated in Figure 3.

The proposed method needs a nonlinear dynamic FE model for LS-DYNA in the analysis domain and a linear static FE model for NASTRAN in the design domain. The two FE models should match and the nonlinear dynamic FE model is generally converted to a linear static model. Recently, the converting process was released by a commercial software system that is ESL-DYNA in GENESIS (Vanderplaats Research and Development, Inc., 2014). The detailed procedure of the proposed method is presented in Figure 4 and the steps of the method are as follows:

Step 1. Set the initial design variables and the cycle number k by zero: $\mathbf{b}^{(k)} = \mathbf{b}^{(0)}$.

Step 2. Perform nonlinear dynamic analysis and extract the displacement $z_{\text{N,roof}}\big|_{t=\text{arbitrary}}$ at the grids of the area that includes the contact area between the roof and the rigid wall. The area should cover the probable contact area.

Step 3. Perform linear static analysis with the enforced displacement using $z_{\text{N,roof}}\big|_{t=\text{arbitrary}}$.

Step 4. Calculate the correction factor α from Equation (3)

Step 5. Solve the following linear static response structural optimization problem in the design domain:

$$\text{Find} \quad \mathbf{b} \in R^n \tag{4}$$

$$\text{to minimize} \quad \text{mass} \tag{5}$$

$$\text{subject to} \quad \mathbf{K}_{\text{L}}\left[\mathbf{z}_{\text{L,residual}},\ \mathbf{z}_{\text{N}}\big|_{t=\text{arbitrary}}\right]^{\text{T}} = \left[\mathbf{0},\ \mathbf{f}\right]^{\text{T}} \tag{6}$$

$$\sum \hat{\mathrm{F}}_{\text{reaction force}}(\mathbf{z}_{\text{N,roof}}\big|_{t=\text{arbitrary}}) \geq \mathrm{F}_{\text{minimum}} \tag{7}$$

where $\mathbf{K}_{\text{L}}$ is the linear stiffness matrix and $\mathbf{f}$ is the equivalent load vector that imposes the enforced displacements $\mathbf{z}_{\text{N,roof}}\big|_{t=\text{arbitrary}}$. Equation (6) represents the governing equation of finite element analysis with the enforced displacement vector $\mathbf{z}_{\text{N,roof}}\big|_{t=\text{arbitrary}}$. $\sum \hat{\mathrm{F}}_{\text{reaction force}}$ is the corrected sum of the reaction forces and $\mathrm{F}_{\text{minimum}}$ is the minimum force requirement of the regulation. $\sum \hat{\mathrm{F}}_{\text{reaction force}}$

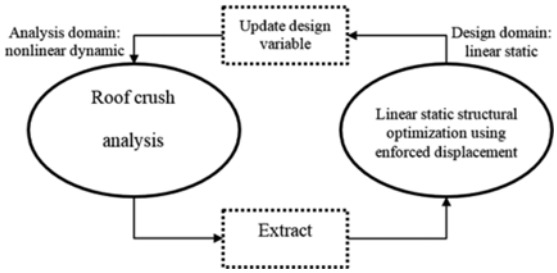

Figure 3. Schematic view of the proposed method.

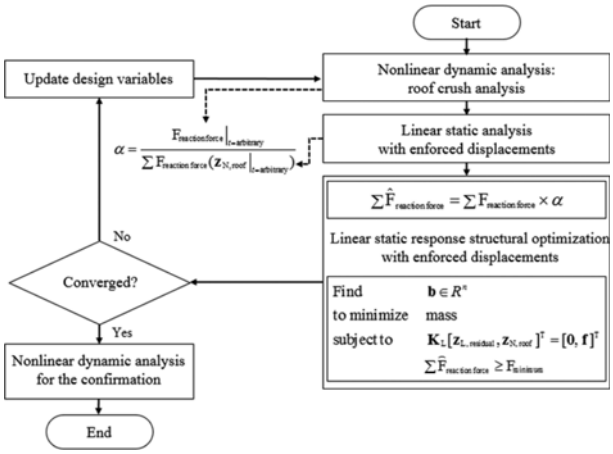

Figure 4. Flow chart of the proposed method.

in Equation (7) has the same value as the rigid wall force from the roof crush analysis, and it is calibrated during the optimization process.

Step 6. If the convergence criterion

$$\left\| \frac{\mathbf{b}^{(k)} - \mathbf{b}^{(k-1)}}{\mathbf{b}^{(k)}} \right\| \leq \varepsilon \tag{8}$$

is satisfied, the process is terminated. Otherwise, update the design variables and go to Step 2.

3. SIMPLIFIED ROOF CRUSH PROBLEM

3.1. Finite Element Model

As mentioned earlier, a simplified roof crush FE model is used to validate the proposed method. The FE model with reinforcement plates is illustrated in Figure 1. The analysis conditions are described in Section 2. The corresponding linear FE model is generated by using ESL-DYNA (Vanderplaats Research and Development, Inc., 2014). In the linear FE model, shell thicknesses, grids, elements and elastic moduli are the same as those of the nonlinear dynamic FE model.

3.2. Optimization of the Simplified Problem

The design formulation is defined using the simplified roof crush finite element model. Twelve design variables are defined by the thicknesses of shell structures as presented in Figure 5. The initial thickness of all the shell structures is 1.80 mm, and the lower bounds and upper bounds of all the design variables are 0.05 mm and 25.00 mm, respectively. The design constraint of the rigid wall force is defined based on the peak value of the rigid wall force. Thus, only one time step is considered for the peak time of the rigid wall force. In the initial FE model, the peak value of the rigid wall force is 201 kN at 1.748 s in Figure 2 and the design constraint for the peak value of the rigid wall force is defined by an arbitrary larger value than 201 kN. The objective function is the mass and the design formulation of the simplified roof crush test is as follows:

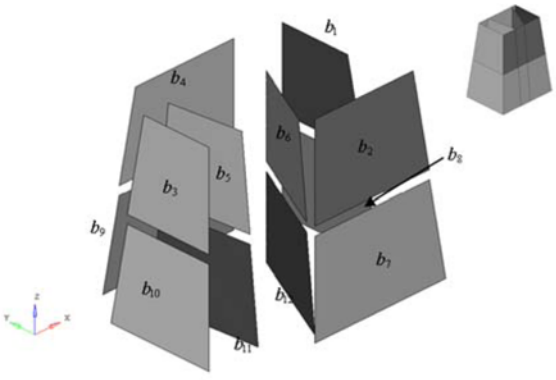

Figure 5. Design variables for the simplified roof crush model.

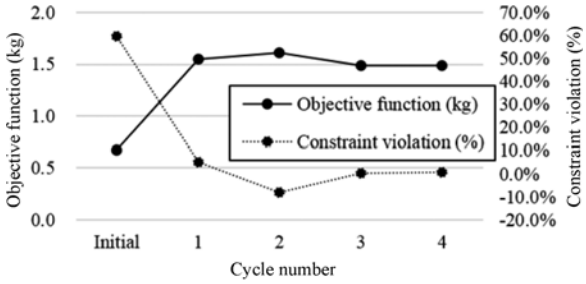

Figure 6. History of the objective function and the constraint violation.

$$\text{Find} \quad b_i;\ i = 1, 2, ..., 12 \tag{9}$$

$$\text{to minimize} \quad \text{mass} \tag{10}$$

$$\text{subject to} \quad \sum \hat{F}_{\text{reaction force}}(\mathbf{z}_N|_{t=\text{peak}}) \geq 500 \text{ kN} \tag{11}$$

$$0.50 \text{ mm} \leq b_i \leq 25.00 \text{ mm} \tag{12}$$

where b_i is ith design variable and $\sum \hat{F}_{\text{reaction force}}(z_N|_{t=\text{peak}})$ is the peak value of the rigid wall force. Figure 6 illustrates the history of the objective function and the constraint violation. In the initial design cycle, the peak force is 201 kN. Therefore, the constraint violation is 59.8 % and mass is 0.675 kg. The simplified FE model converges in the 4th design cycle, and this means that the optimum results are obtained by nonlinear dynamic analyses executed 5 times. The mass is increased to 1.489 kg while the design constraint is satisfied. Since the design constraint is violated in the initial model, the mass is increased. Figure 7 shows the rigid wall force of the initial model and the optimum model. As mentioned before, the peak force occurs at 1.748 s with 201 kN. At the optimum, the peak force occurs at 1.448 s with 497 kN. The thicknesses of the initial model and the optimum model are compared in Table 2. The design variables 5, 6, 11, 12 are for the reinforcements, and they become thicker than the others. The reinforcements are parallel with respect to the z-direction. Therefore, the structures in the normal direction of the rigid wall have more influence on the rigid wall force.

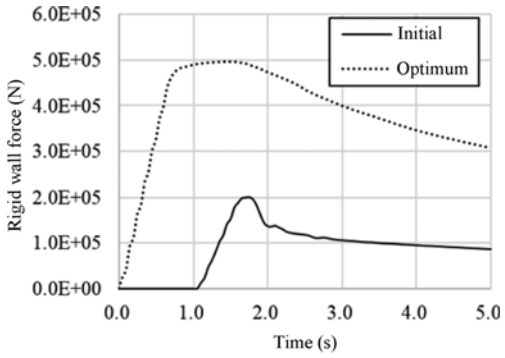

Figure 7. Comparison the rigid wall force of the initial model and the optimum model.

Table 2. Comparison between the initial thickness and the optimum thickness of the simplified model.

Design variables	Initial	Optimum
b_1	1.800	4.195
b_2	1.800	4.033
b_3	1.800	4.216
b_4	1.800	4.019
b_5	1.800	4.811
b_6	1.800	4.723
b_7	1.800	3.386
b_8	1.800	3.484
b_9	1.800	3.388
b_{10}	1.800	3.530
b_{11}	1.800	4.384
b_{12}	1.800	4.153

4. ROOF CRUSH PROBLEM

4.1. Finite Element Model for FMVSS 216 Regulation

The purpose of FMVSS 216 is to reduce deaths and injuries due to the crushing of the roof into the passenger compartment in rollover accidents, and the regulation was established by DOT National Highway Traffic Safety Administration (2009). The fatality rate is greater than for other types of accidents such as frontal impact crash, because there are no specific devices to absorb the impact energy between the roof and the passenger. Minimum roof strength is regulated under FMVSS 216 for the roof of passenger cars, multipurpose passenger vehicles, trucks and buses with a gross vehicle weight rate (GVWR) of 4,536 kg or less. If the GVWR is less than 2,722 kg, the minimum roof strength is 3 times the empty weight of the vehicle, and if GVWR is greater than 2,722 kg the minimum roof strength is 1.5 times the empty weight of the vehicle.

Figure 8 shows the static loading device for FMVSS 216. The device consists of a rigid horizontal support system and the rigid wall with its lower surface formed as a flat rectangle 762 mm by 1,829 mm. The force is applied in a normal direction to the lower flat surface of the rigid wall at 13 mm/s until it reaches 127 mm. Thus, when the rigid wall displacement reaches 127 mm, the rigid wall force should satisfy the minimum force. The vehicle's sills are placed on a rigid horizontal support system and fixed rigidly. The direction of the rigid wall is rotated at a 25 degree roll angle and a 5 degree pitch angle.

In this research, a full scale FE vehicle model is utilized to validate the proposed method. The FE model for a commercial vehicle is illustrated in Figure 9. The model was developed and validated by the National Crash Analysis Center (NCAC) of George Washington University (Jeong *et al*., 2008). The total number of elements is 432,596 and the total number of nodes is 431,629. The roof crush analysis using the FE model is conducted under the conditions specified in FMVSS 216. The vehicle sills are fixed using boundary conditions.

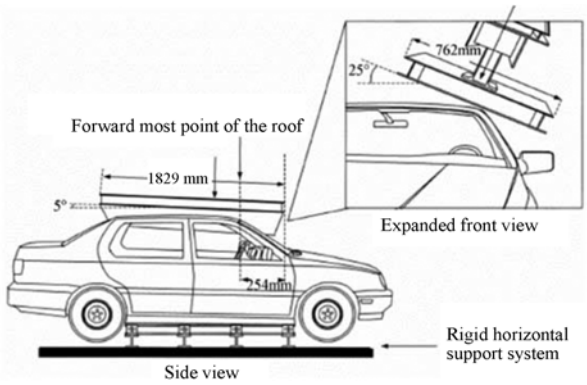

Figure 8. Static loading device for FMVSS 216.

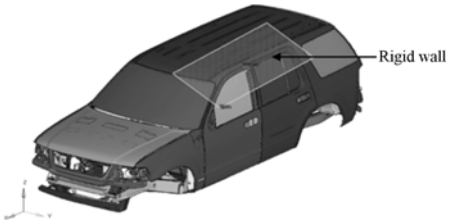

Figure 9. Finite element model for the full vehicle.

4.2. Roof Crush Optimization

The design formulation of FMVSS 216 is as follows:

$$\text{Find} \quad \mathbf{b} \in R^n \tag{13}$$

$$\text{minimize} \quad \text{mass} \tag{14}$$

$$\text{subject to} \quad F_{\text{rigid wall force}}\big|_{d_{\text{roof}}=127\ \text{mm}} \geq 3.0 \times \text{weight}_{\text{vehicle}} \tag{15}$$

where **b** is the design variable vector and the objective function is the mass of the structure. $F_{\text{rigid wall force}}$ is the rigid wall force when the displacement of roof d_{roof} reaches 127 mm due to crush. $\text{weight}_{\text{vehicle}}$ is the empty weight of the vehicle.

Jeong *et al*. (2008) compared the performance of ESLM and metamodel based optimization regarding the roof crush optimization using a full scale vehicle. ESLM greatly reduced the number of crash analyses compared to the metamodel based optimization and the optimum mass using ESLM is smaller than the optimum mass obtained by the metamodel approach. However, ESLM cannot consider the design constraint of the rigid wall force because the rigid wall force is a response from nonlinear dynamic analysis. Therefore, the design constraint of the rigid wall force is converted to a displacement constraint in linear

static structural optimization as follows:

$$\text{Find} \quad b_i;\ i = 1, 2, ..., 9 \tag{16}$$

$$\text{minimize} \quad \text{mass} \tag{17}$$

$$\text{subject to} \quad d_{roof} \le 127 \text{ mm} \tag{18}$$

$$0.6 \text{ mm} \le b_i \le 4.0 \text{ mm} \tag{19}$$

where b_i is the ith design variable. The rigid wall force constraint in Equation (15) is converted to the displacement constraint in Equation (18).

Figure 10 shows the force-displacement curves that are extracted from the roof crush test. The FE model in Figure 9 is named as the initial model, and the force-displacement curve of the commercial vehicle is the solid line in Figure 10. It is noted the rigid wall force of the initial model does not satisfy the minimum strength at the displacement of 127 mm in Equation (15). A desired force-displacement curve is found by a trial-and-error process by changing the thicknesses of the structure, and this changed model is named as the modified model. The force-displacement curve of the modified model is depicted by a dotted line in Figure 10. The ESLM process should start with the modified model. In other words, roof crush optimization should start from the feasible region. Actually, the force-displacement curve is a response, not an external load. The force-displacement curve is changed to a force-time curve and the force-time curve is imposed on the rigid wall as a point external load, and does not change during the design cycle. Even if the force-time curve is unchanged during the optimization cycles, the force-displacement curve can be changed according to the design change. Therefore, after the ESLM process converges, roof crush analysis should be performed again to confirm that Equation (15) is satisfied. In this case, the optimization result can either be over design or cannot satisfy the design constraint. These are the drawbacks of the roof crush optimization using ESLM.

To overcome the above drawbacks, a novel method for roof crush optimization is proposed. The results are compared with ESLM and the proposed method. The

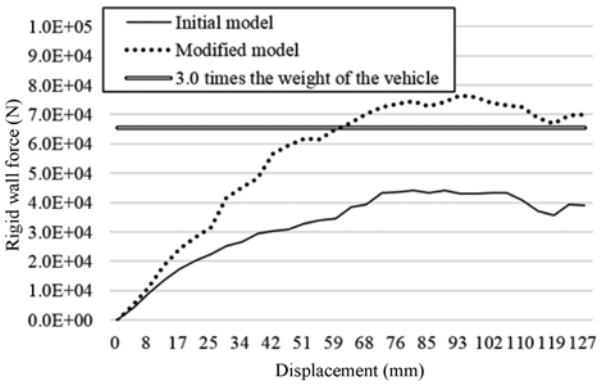

Figure 10. Comparison of the initial model and the modified model.

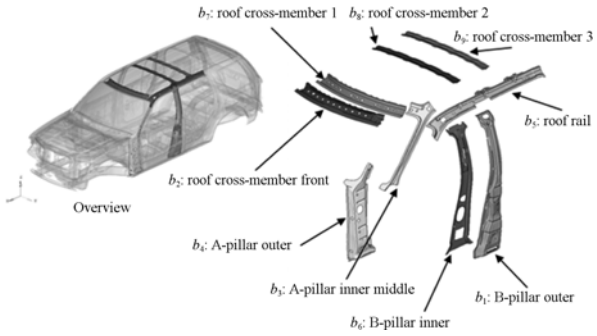

Figure 11. Design variables for the roof crush optimization.

design formulation is as follows:

$$\text{Find} \quad b_i;\ i = 1, 2, ..., 9 \tag{20}$$

$$\text{minimize} \quad \text{mass} \tag{21}$$

$$\text{subject to} \quad \sum \hat{F}_{\text{reaction force}}\Big|_{d_{roof}=127 \text{ mm}} \ge 65{,}386 \text{ N} \quad (= 3.0 \times \text{weight}_{\text{vehicle}}) \tag{22}$$

$$0.6 \text{ mm} \le b_i \le 4.0 \text{ mm} \tag{23}$$

Figure 11 shows the nine design variables, which are selected based on the report of Jeong *et al*. (2008). The objective function is the mass and the rigid wall force constraint 65,386 N is obtained from 3 times of the vehicle weight (2,224 kg × 9.8 m/s^2). To validate the proposed method, the optimization starts from the feasible region and the infeasible region. Using the previous modified model, optimization can start from the feasible region. Optimization can start from the infeasible region using the initial FE model in Figure 9 and the constraint violation is 40.1 %. As mentioned before, the initial thicknesses of both models are shown in Table 3. In linear static response

Table 3. Thicknesses of the initial model and the modified model.

Design variables	Thickness (mm)	
	Initial model	Modified model
b_1	1.20	2.80
b_2	1.10	2.80
b_3	1.00	2.80
b_4	0.85	2.80
b_5	2.25	2.80
b_6	2.24	2.80
b_7	1.36	2.80
b_8	1.30	2.80
b_9	1.00	2.80
Mass	17.71 kg	38.23 kg

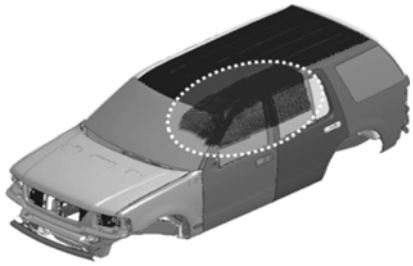

Figure 12. Selected grids for enforced displacements.

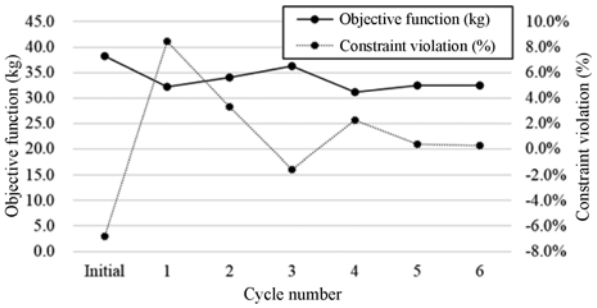

Figure 13. History of the objective function and constraint violation: Starting from the feasible region.

structural optimization, external loads are the enforced displacements that are the displacements from the roof crush analysis. Displacements are obtained for all degrees of freedom of the selected grids. The grids in the contacted area between the roof and rigid wall should be a subset of the selected grids. The selected grids are illustrated in Figure 12.

As illustrated in Figure 13, the proposed method converges in the 6th design cycle when starting from the feasible region using the previous modified model. The mass is decreased from 38.23 kg to 32.45 kg while the rigid wall force constraint is satisfied. The rigid wall force of the optimum model is 65198.4 N when the rigid wall displacement reaches 127 mm. Figure 14 illustrates the force-displacement curve of the modified model and the optimum model. The optimization process which starts from the infeasible region converges in the 13th design cycle. Figure 15 presents the history of the objective

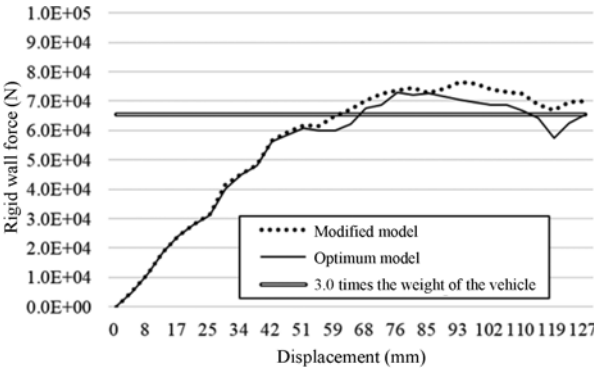

Figure 14. Comparison of the modified model and the optimum model: Starting from the feasible region.

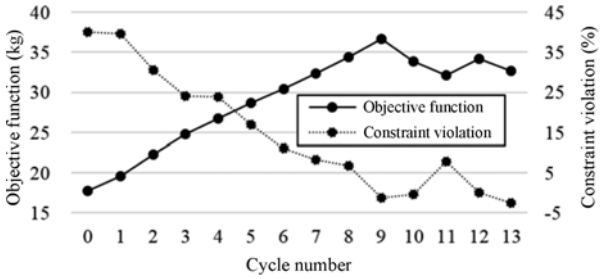

Figure 15. History of the objective function and the constraint violation: Starting from the infeasible region.

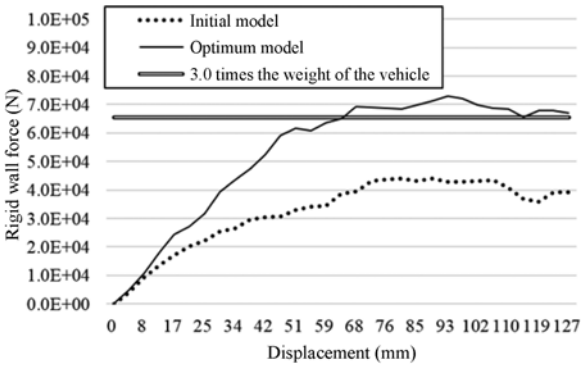

Figure 16. Comparison of the modified model and the optimum model: Starting from the infeasible region.

Table 4. Comparison of the optimization results.

		b_1	b_2	b_3	b_4	b_5	b_6	b_7	b_8	b_9	Mass (kg)	No. of analyses
ESLM		4.00	4.00	4.00	4.00	3.77	1.00	1.63	1.00	1.00	34.28	14
Proposed method starting from	Feasible region	4.00	3.15	2.13	0.60	1.53	0.60	2.91	3.46	0.60	32.70	7
	Infeasible region	3.66	2.58	2.53	0.60	2.01	0.60	2.76	3.06	2.22	32.45	14

function and constraint violation. The mass is increased from 17.71 kg to 32.70 kg because the initial FE model violates the minimum strength by 40.1 %. The rigid wall force of the optimum model is 67,025.2 N when the rigid wall displacement reaches 127 mm. Figure 16 illustrates the force-displacement curve of the initial FE model and the optimum model.

Table 4 compares the optimization results of the proposed method and ESLM. The optimum results of ESLM are from Jeong *et al*. (2008). ESLM needs 14 nonlinear roof crush analyses and the optimum mass is 34.28 kg. The design starts from the feasible region using the modified model. The proposed method needs 7 nonlinear roof crush analyses when starting from the feasible region. Furthermore, the optimum mass for the proposed method is 1.58 kg lighter than for ESLM. If the design starts from the infeasible region and 14 nonlinear roof crush analyses are needed. The optimum mass is 32.45 kg. The number of analyses is exactly the same with ESLM. However, the mass is 1.83 kg lighter. It is noted that ESLM cannot start from the infeasible region. The proposed method provides an excellent solution even when the design starts from the infeasible region.

5. CONCLUSION

In this research, a novel nonlinear dynamic structural optimization method is proposed for the roof crush problem and validated using a full scale vehicle FE model. The proposed method repeats the analysis domain and the design domain until the convergence criteria are satisfied. In the design domain, enforced displacements are utilized to generate as external loads that are obtained for the grids of the roof area. The difference of the rigid wall force from the roof crash analysis and the sum of the reaction forces at the boundary conditions is calibrated using the correction factor. The results are compared with the results from ESLM and concluding remarks are made as follows:

(1) The proposed method significantly reduces the number of nonlinear dynamic analyses.
(2) The rigid wall force constraint can be considered indirectly in linear static structural optimization using the correction factor.

The proposed method can consider many design variables and a full scale vehicle. However, IIHS proposed a new condition for roof strength, which is a more severe condition than FMVSS 216. In future works, the proposed method will be extended to include the new regulations of IIHS.

ACKNOWLEDGEMENT–This work was supported by the Korea Science and Engineering Foundation (KOSEF) grant funded by the Korea government (MEST) (No. 2017R1A2B4004480, 2017R1A6A3A11030427). and the National Institute of Supercomputing and Network/Korea Institute of Science and Technology Information with supercomputing resources including technical support (KSC-2016-S1-0010). The authors are thankful to Mrs. MiSun Park for her English correction of the manuscript.

REFERENCES

Cho, Y. H. and Han, B. K. (2012). Roof strength performance improvement enablers. *Int. J. Automotive Technology* **13**, **5**, 775–781.

Choi, W. S. and Park, G. J. (1999). Transformation of dynamic loads into equivalent static loads based on modal analysis. *Int. J. Numerical Methods in Engineering* **46**, **1**, 29–43.

DOT National Highway Traffic Safety Administration (2009). FMVSS No. 216a, Roof Crush Resistance.

Green, N. S., Canfield, R. A., Swenson, E. D., Yu, W. and Blair, M. (2009). Structural optimization of joined-wing beam model with bend-twist coupling using equivalent static loads. *50th AIAA/ASME/ASCE/AHS Structures, Structural Dynamics, and Materials Conf*., Palm Springs, California, USA.

Hong, E. P., You, B. J., Kim, C. H. and Park, G. J. (2010). Optimization of flexible components of multibody systems via equivalent static loads. *Structural and Multidisciplinary Optimization* **40**, **1-6**, 549–562.

Jang, H. H., Lee, H. A., Lee, J. Y. and Park, G. J. (2012). Dynamic response topology optimization in the time domain using equivalent static loads. *AIAA Journal* **50**, **1**, 226–234.

Jang, H. H., Lee, Y. and Park, G. J. (2016). Optimization of the loading path for the tube-hydroforming process. *Proc. Institution of Mechanical Engineers, Part D: J. Automobile Engineering* **230**, **12**, 1605–1623.

Jeong, S. B., Yi, S. I., Kan, C. D., Nagabhushana, V. and Park, G. J. (2008). Structural optimization of an automobile roof structure using equivalent static loads. *Proc. Institution of Mechanical Engineers, Part D: J. Automobile Engineering* **222**, **11**, 1985–1995.

Jeong, S. B., Yoon, S., Xu, S. and Park, G. J. (2010). Nonlinear dynamic response structural optimization of an automobile frontal structure using equivalent static loads. *Proc. Institution of Mechanical Engineers, Part D: J. Automobile Engineering* **224**, **4**, 489–501.

Kahane, C. J. (1989). *An Evaluation of Door Locks and Roof Crush Resistance of Passenger Cars, Federal Motor Vehicle Safety Standards 206 and 216*. National Highway Traffic Safety Administration. Washington DC, USA.

Kim, Y. I. and Park, G. J. (2010). Nonlinear dynamic response structural optimization using equivalent static loads. *Computer Methods in Applied Mechanics and Engineering* **199**, **9**, 660–676.

Lee, H. A. and Park, G. J. (2015). Nonlinear dynamic response topology optimization using the equivalent static loads method. *Computer Methods in Applied Mechanics and Engineering*, **283**, 956–970.

Lee, S. J., Lee, H. A., Yi, S. I., Kim, D. S., Yang, H. W. and

Park, G. J. (2013). Design flow for the crash box in a vehicle to maximize energy absorption. *Proc. Institution of Mechanical Engineers, Part D: J. Automobile Engineering* **227**, **2**, 179–200.

Lee, Y., Yoon, J. M. and Park, G. J. (2016). A novel method for roof crush optimization using enforced displacements. *Asian Cong. Structural and Multidisciplinary Optimization*, Nagasaki, Japan.

Lim, J. H., Park, J. S., Yun, Y. W., Jeong, S. B. and Park, G. J. (2015). Design of an airbag system of a mid-sized automobile for pedestrian protection. *Proc. Institution of Mechanical Engineers, Part D: J. Automobile Engineering* **229**, **5**, 656–669.

Livermore Software Technology Co. (2007). LS-DYNA User's Manual.

Mao, M., Chirwa, E. and Chen, T. (2007). Reinforcement of vehicle roof structure system against rollover occupant injuries. *Int. J. Crashworthiness* **12**, **1**, 41–55.

MSC Software Co. (2013). NASTRAN User's Guide.

Müllerschön, H., Erhart, A. and Schumacher, P. (2013). Topology and topometry optimization of crash applications with the equivalent static load method. *10th World Cong. Structural and Multidisciplinary Optimization*, Orlando, Florida, USA.

Niknejad, A., Abdolzadeh, Y., Rouzegar, J. and Abbasi, M. (2015). Experimental study on the energy absorption capability of circular corrugated tubes under lateral loading and axial loading. *Proc. Institution of Mechanical Engineers, Part D: J. Automobile Engineering* **229**, **13**, 1739–1761.

Pan, F. and Zhu, P. (2011). Design optimisation of vehicle roof structures: Benefits of using multiple surrogates. *Int. J. Crashworthiness* **16**, **1**, 85–95.

Park, G. J. (2011). Technical overview of the equivalent static loads method for non-linear static response structural optimization. *Structural and Multidisciplinary Optimization* **43**, **3**, 319–337.

Rechnitzer, G., Lane, J. and Scott, G. (1996). Rollover crash study – Vehicle design and occupant injuries. *15th Int. Technical Conf. Enhanced Safety of Vehicles*, Melbourne, Victoria, Australia.

Seo, J. H., Lee, E. D., Lee, J. W. and Han, B. K. (2016). Effect of tumble-home on roof strength of a vehicle. *Int. J. Automotive Technology* **17**, **4**, 665–670.

Strashny, A. (2007). An Analysis of Motor Vehicle Rollover Crashes and Injury Outcomes. Report DOT HS 810 741. National Highway Traffic Safety Administration.

Tey, J. Y., Ramli, R. and Abdullah, A. S. (2016). A new multi-objective optimization method for full-vehicle suspension systems. *Proc. Institution of Mechanical Engineers, Part D: J. Automobile Engineering* **230**, **11**, 1443–1458.

Vanderplaats Research and Development, Inc. (2014). GENESIS User's Manual Version 13.1 Design Reference.

Wang, C. Q., Wang, D. F. and Zhang, S. (2016). Design and application of lightweight multi-objective collaborative optimization for a parametric body-in-white structure. *Proc. Institution of Mechanical Engineers, Part D: J. Automobile Engineering* **230**, **2**, 273–288.

Yi, S. I., Lee, J. Y. and Park, G. J. (2012). Crashworthiness design optimization using equivalent static loads. *Proc. Institution of Mechanical Engineers, Part D: J. Automobile Engineering* **226**, **1**, 23–38.

Yun, Y. W., Choi, J. S. and Park, G. J. (2014). Optimization of an automobile curtain airbag using the design of experiments. *Proc. Institution of Mechanical Engineers, Part D: J. Automobile Engineering* **228**, **4**, 370–380.